

Supporting Information

Ultrasound-triggered *in situ* gelation with ROS-controlled drug release for cartilage repair

Shunli Wu,^{a,b,c,d†} Hao Zhang,^{a,b†} Sicheng Wang,^{a,b,c†} Jinru Sun,^{a,b,c} Yan Hu,^{a,b,f} Han Liu,^{a,b} Jinlong Liu,^{a,b} Xiao Chen,^g Fengjin Zhou,^{h*} Long Bai,^{a,b*} Xiuhui Wang,^{a,b*} Jiaca Su,^{a,b*}

^aInstitute of Translational Medicine, Shanghai University, Shanghai 200444, China

^bOrganoid Research Center, Shanghai University, Shanghai, 200444 China

^cSchool of Medicine, Shanghai University, Shanghai 200444, China

^dSchool of Environmental and Chemical Engineering, Shanghai University, Shanghai 200444, China

^eDepartment of Orthopedics, Shanghai Zhongye Hospital, Shanghai, China

^fShaoxing Institute of Technology at Shanghai University, Shaoxing, 312000, China

^gDepartment of Orthopedics Trauma, Shanghai Changhai Hospital, Naval Medical University, Shanghai, China

^hDepartment of Orthopaedics, Honghui Hospital, Xi'an Jiao Tong University, Xi'an 710000, China

*Address correspondence to: dr.zhoufj@163.com (F. Z.); bailong@shu.edu.cn (L. B.); blackrabbit@shu.edu.cn (X. W.); jiicansu@shu.edu.cn (J. S.)

†These authors contributed equally to this work.

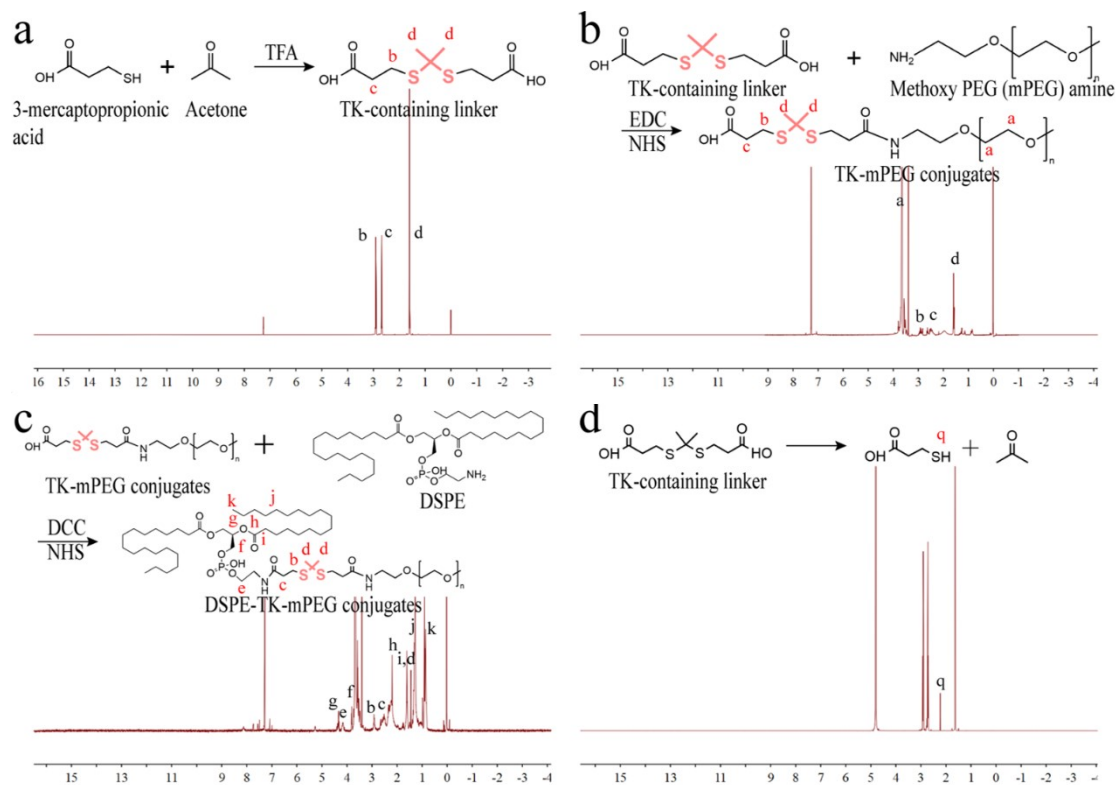


Figure S1. Synthesis and characterization of ROS-responsive precursor. (a-c) The synthesis process and ^1H NMR spectra of the TK linker, TK-mPEG and DSPE-TK-mPEG. (d) The ^1H NMR spectra of the TK broken by H_2O_2 .

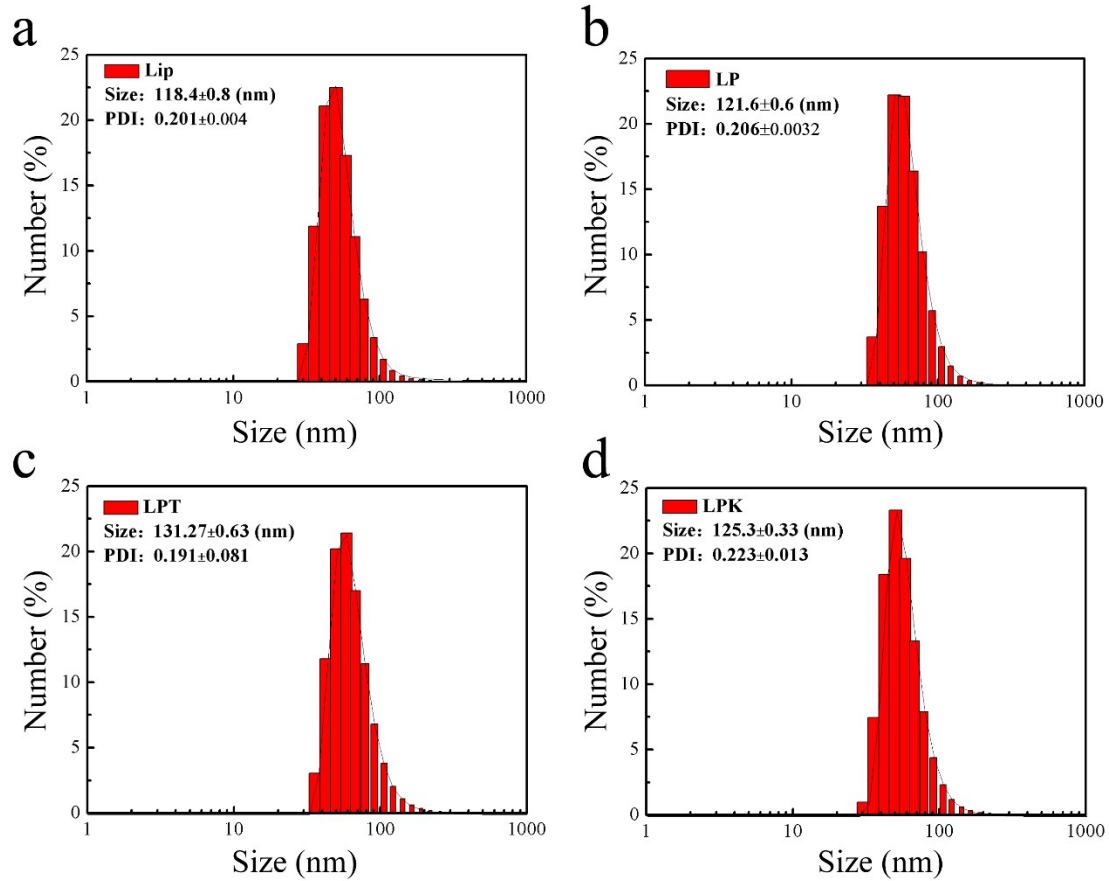


Figure S2. The size of a series of nanoparticles measured by DLS. (a-d) The DLS of Lip, LP, LPT and LPK.

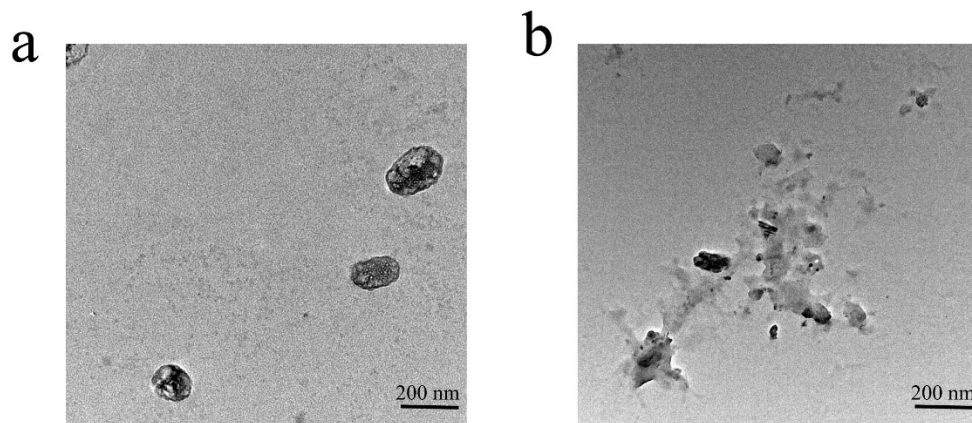


Figure S3. The rupture of LPKT NPs triggered by ROS under US treatment for 3 min. (a) TEM image of Lip NPs with US treatment, (b) TEM image of LPKT NPs with US treatment.

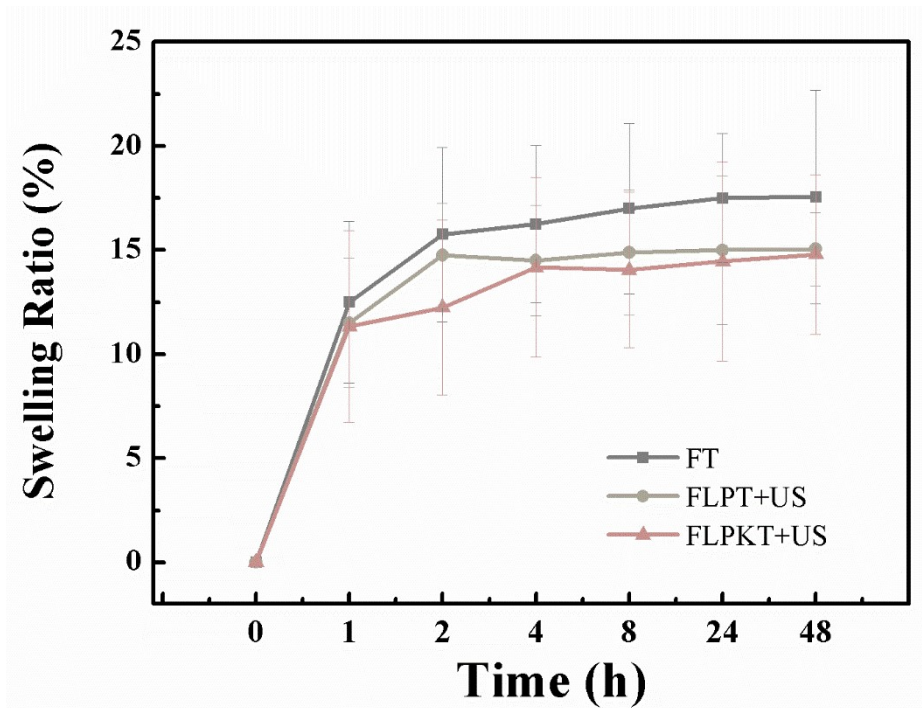


Figure S4. Swelling ratio of nanocomposite hydrogels from initial gelation state to swelling state on the basis of wet hydrogels.

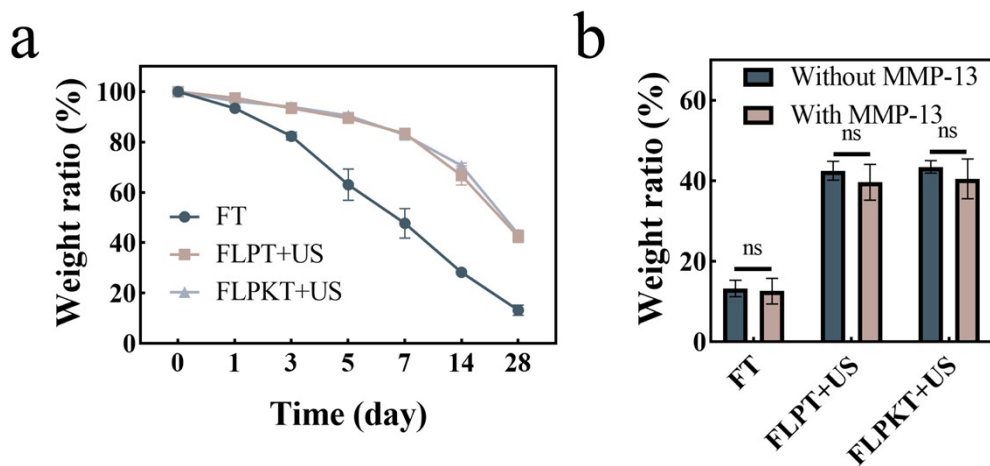


Figure S5. The degradation effect of *in situ* nanocomposite hydrogels in the presence of MMP-13. (a) the overall degradation profile of FT, FLPT+US, and FLPKT+US hydrogels in 25 ng/mL MMP-13 solution for 28 days. (b) The weight rate of *in situ* nanocomposite hydrogels with or without MMP-13 enzyme at day 28.

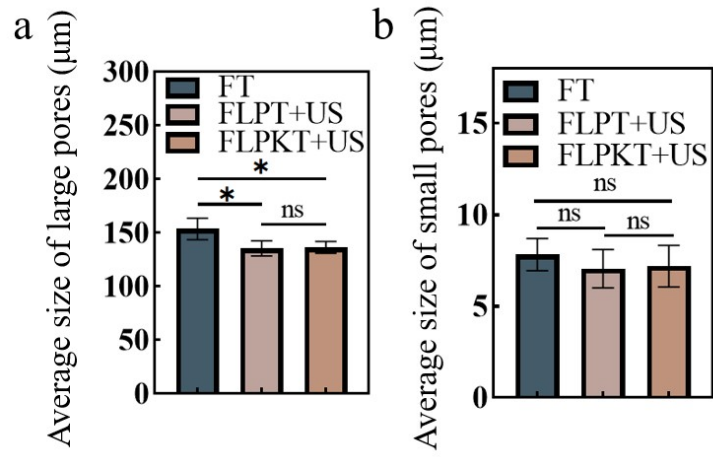


Figure S6. Average sizes of large and small pores in the FT, FLPT+US and FLPKT+US hydrogels. (* $p < 0.05$).

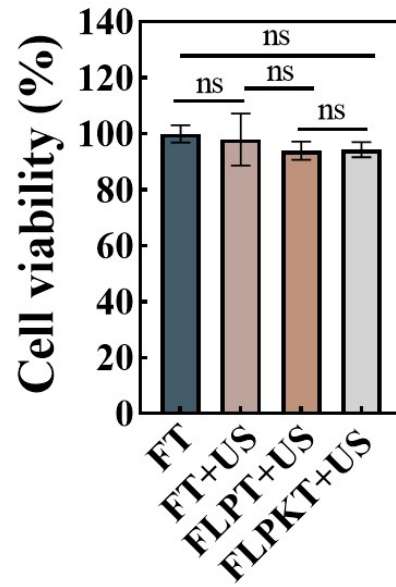


Figure S7. The cell viability of FLPKT+US hydrogels after being cultured for 24 h.

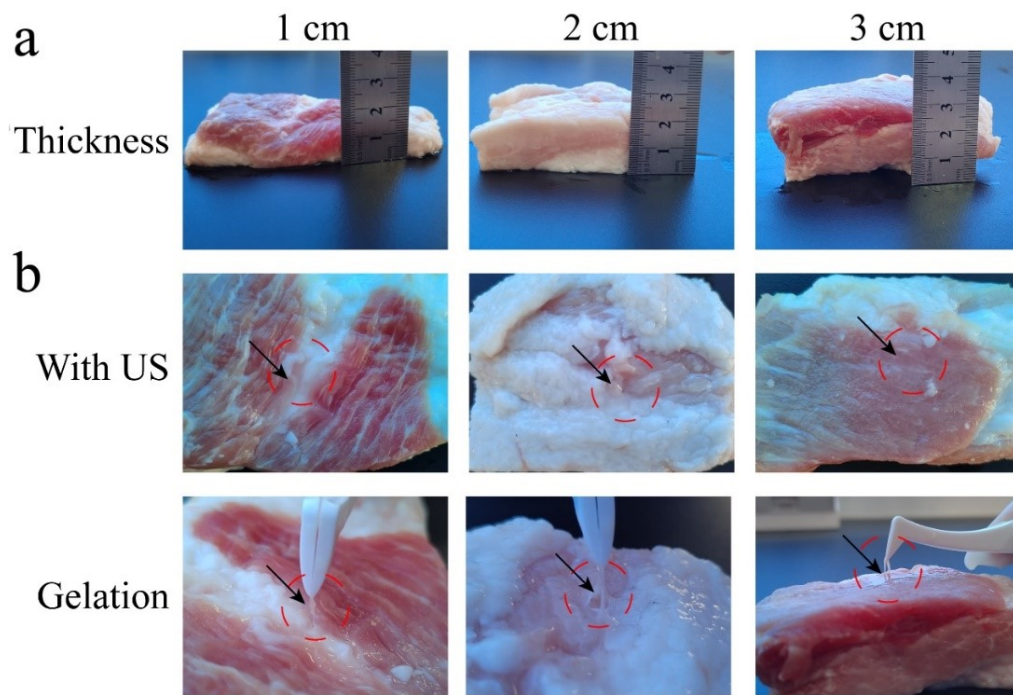


Figure S8. Ultrasonic penetration and gelation capabilities through the pig tissues. (a) The thickness of pig tissues. (b) The effect of surrounding tissues on the capability of gelation under the ultrasonic treatment with 1 MHz, 1 W/cm² for 3 min.

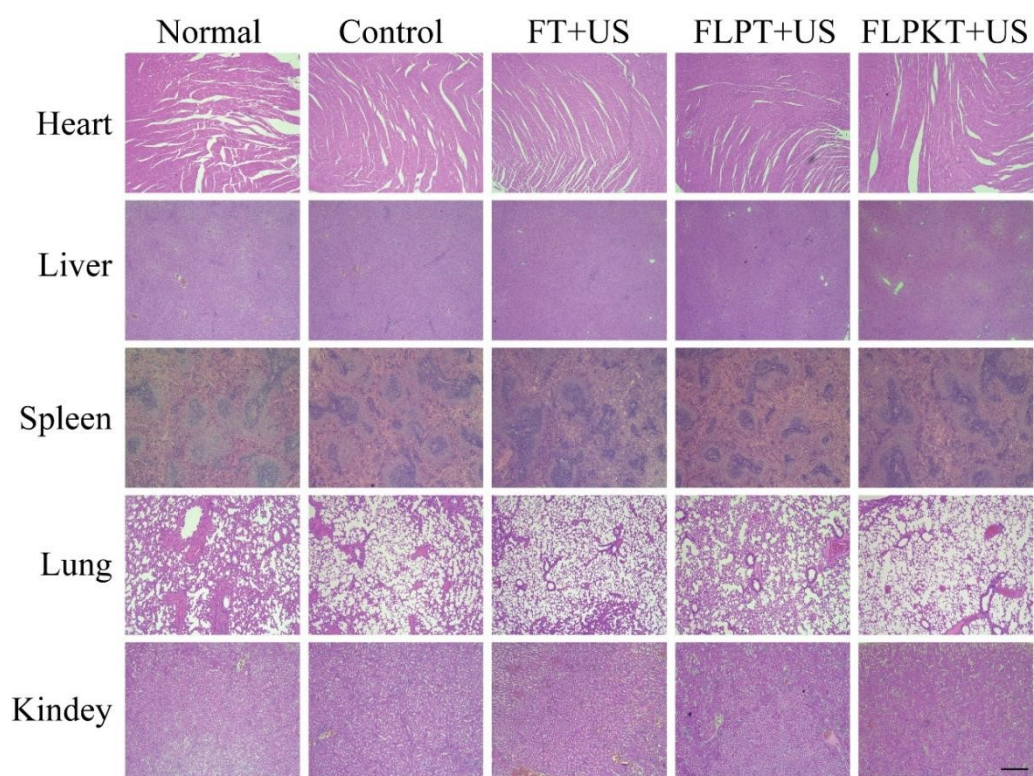


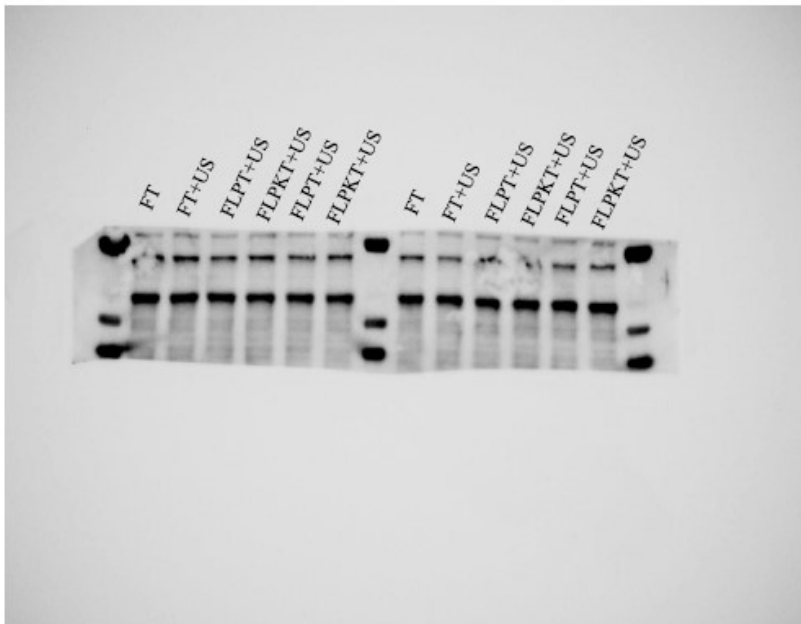
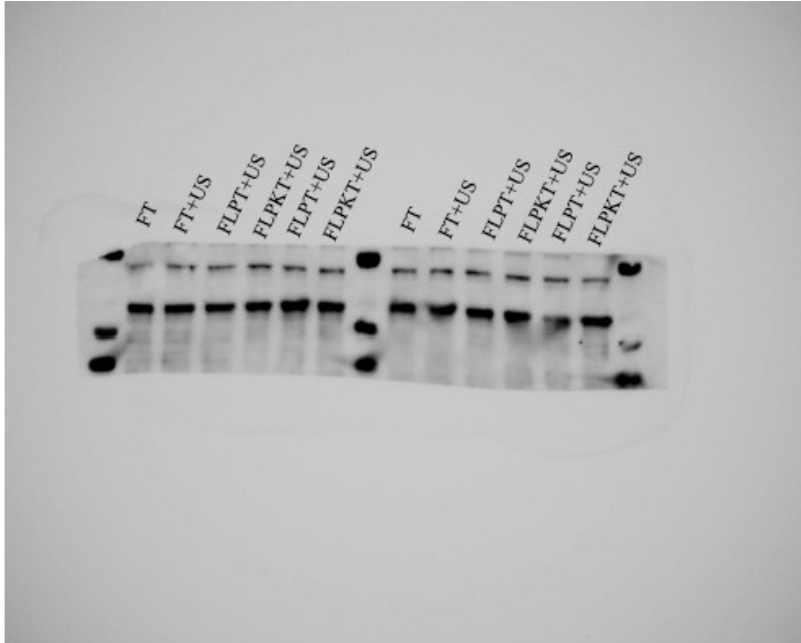
Figure S9. The toxicity of *in situ* nanocomposite hydrogel at 8 weeks. (Scale bar: 500 μm).

Table S1. Primer sequences for qRT-PCR.

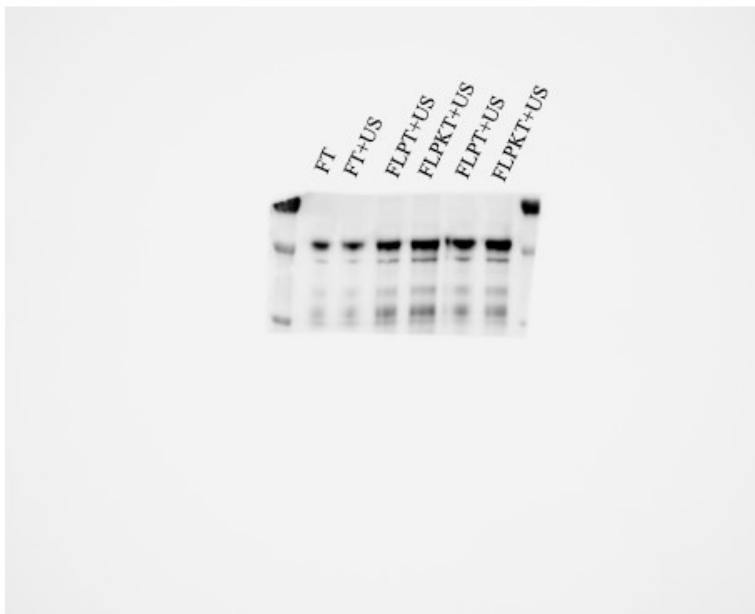
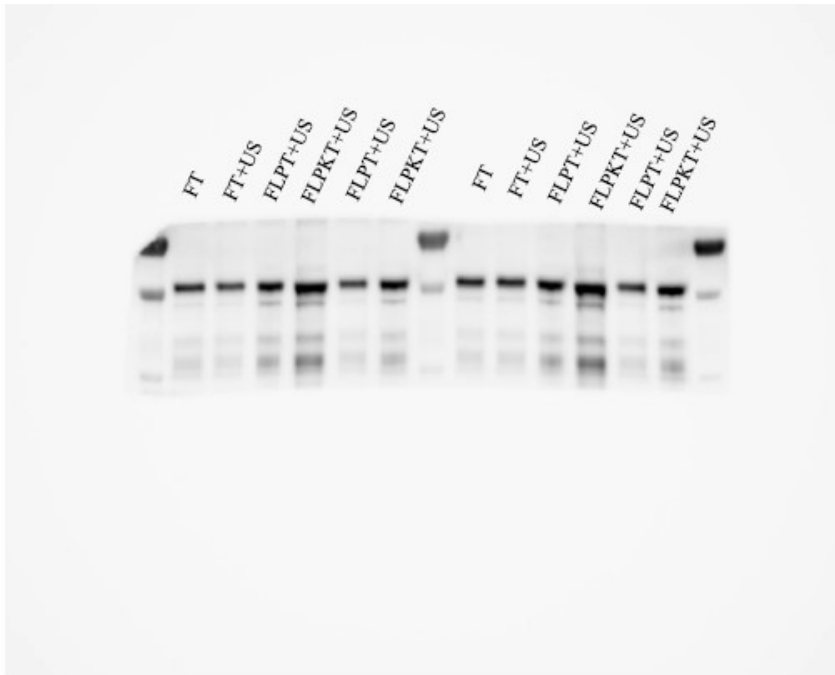
| Gene symbol | 5'-3' |
|-------------|-----------------------|
| GAPDH F | GGTTGTCTCCTGCGACTTCA |
| GAPDH R | TGGTCCAGGGTTTCTTACTCC |
| ACAN F | AACTCAGTGGCCAAACATCC |
| ACAN R | TCAGGAATCCCAGATGTTCC |
| Col2 F | CTCAAGTCGCTGAACAACCA |
| Col2 R | GTCTCCGCTCTTCCACTCTG |
| Sox9 F | TGGCAGAGGGTGGCAGACAG |
| Sox9 R | CGTTGGGCGGCAGGTATTGG |

Western Blot Raw Data and Grouping

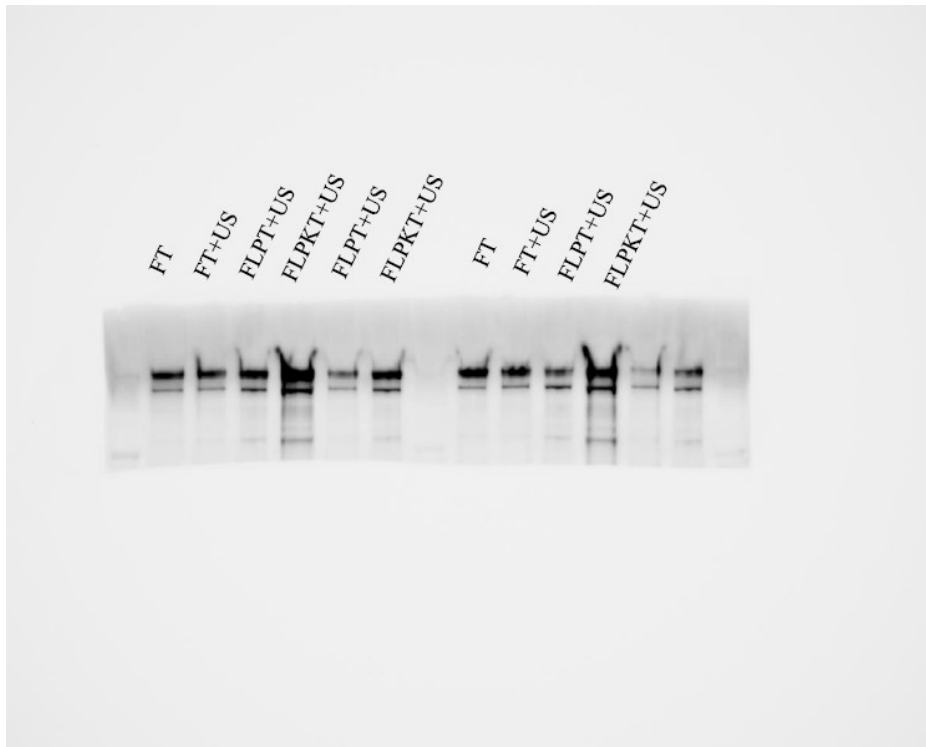
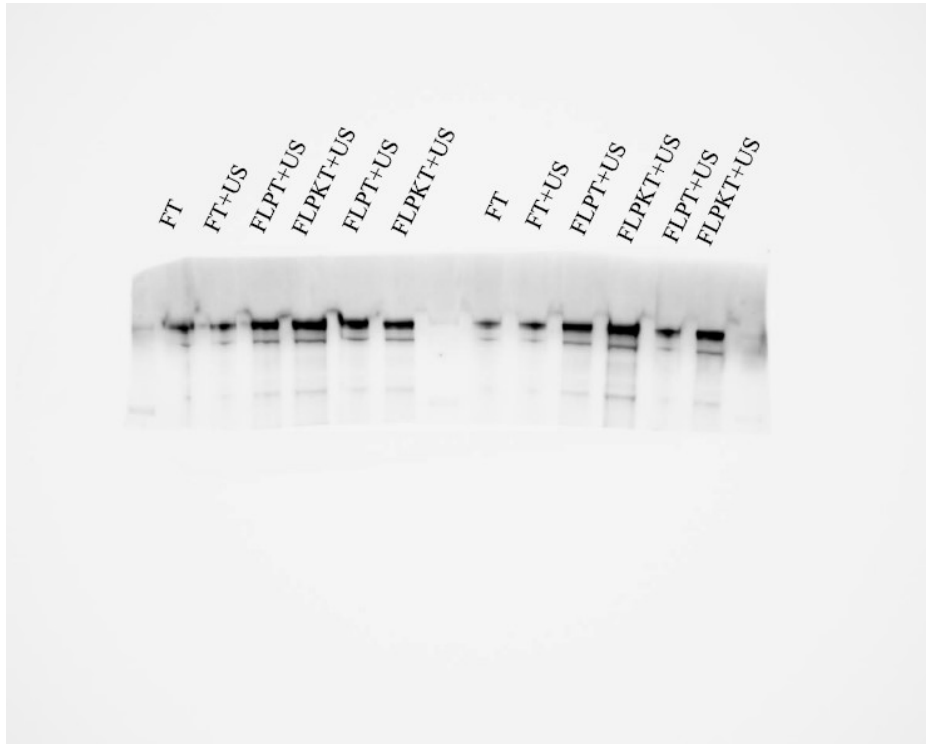
GAPDH



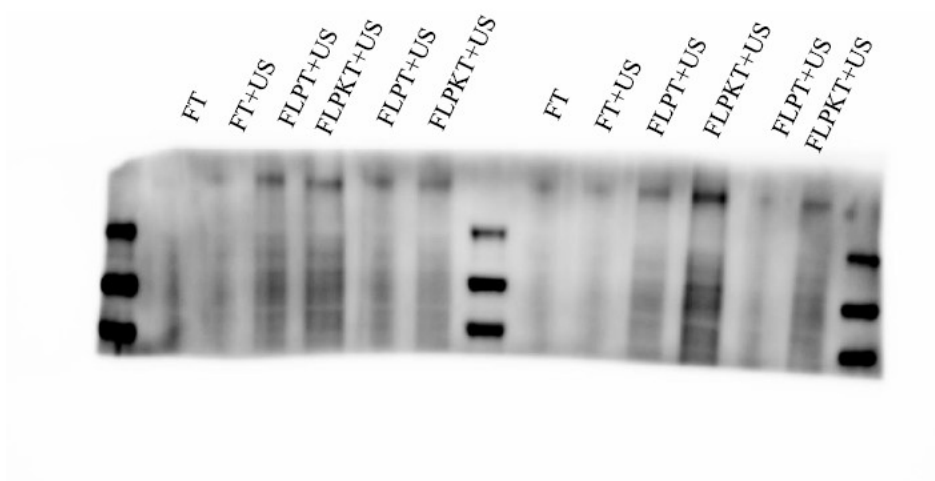
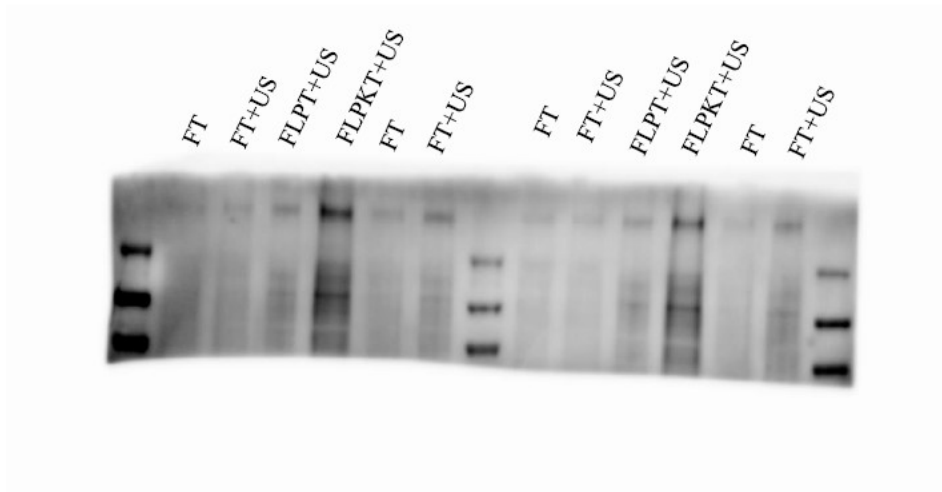
SOX9



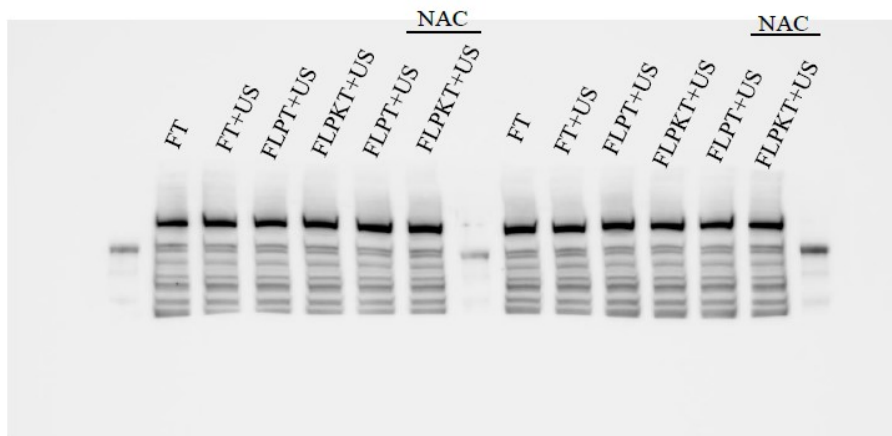
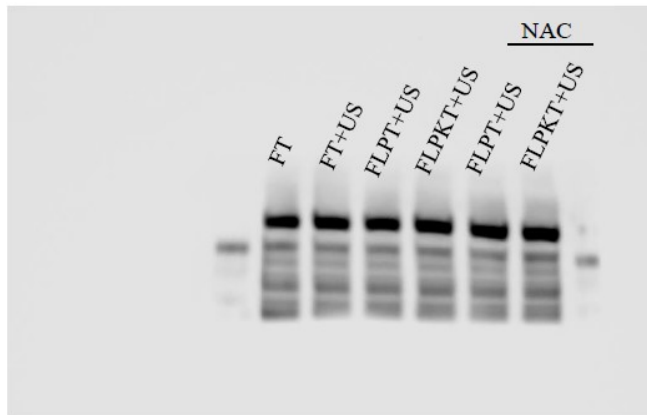
COL II



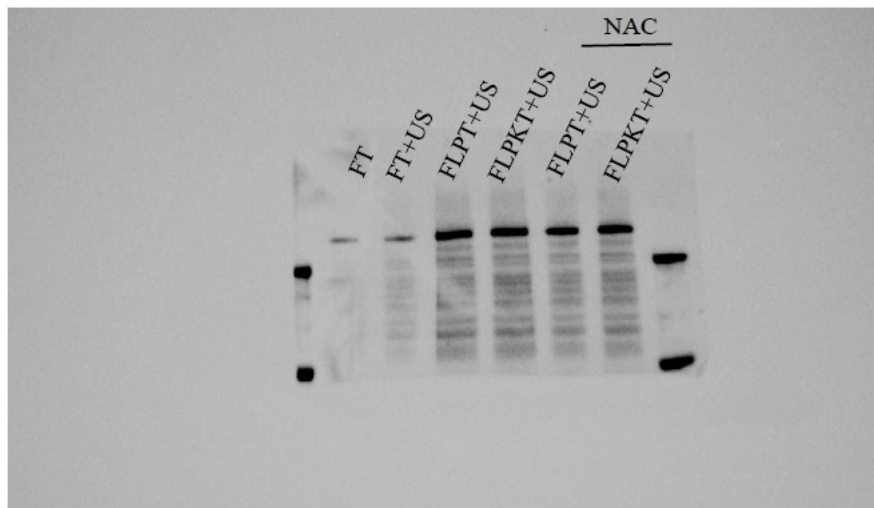
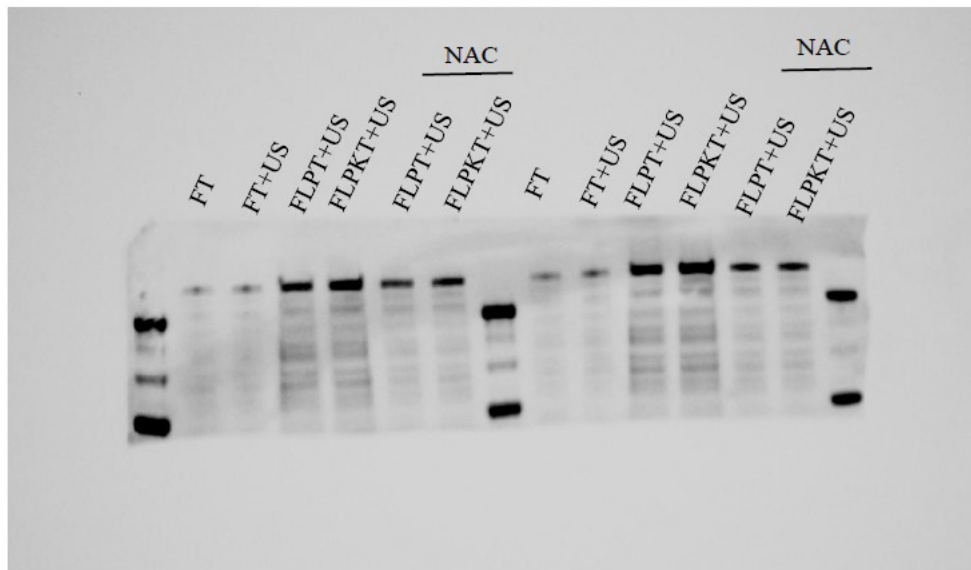
ACAN



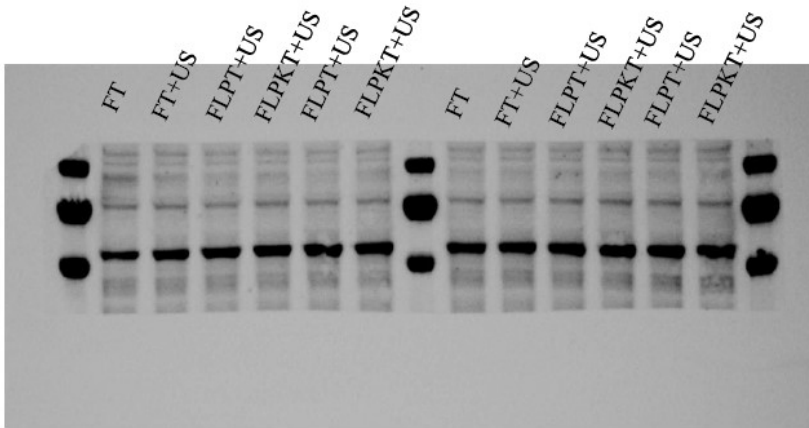
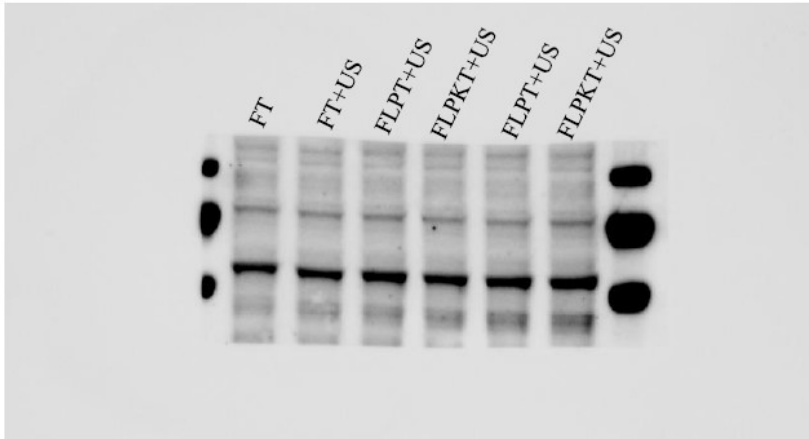
mTOR



p-mTOR



SMAD5



p-SMAD5

